NOTES AND CORRESPONDENCE

Arctic Contribution to Upper-Ocean Variability in the North Atlantic

JOHN E. WALSH AND WILLIAM L. CHAPMAN

Department of Atmospheric Sciences University of Illinois Urbana, Illinois

12 December 1989 and 18 July 1990

ABSTRACT

Because much of the deep water of the world's oceans forms in the high-latitude North Atlantic, the potential climatic leverage of salinity and temperature anomalies in this region is large. Substantial variations of sea ice have accompanied North Atlantic salinity and temperature anomalies, especially the extreme and long-lived "Great Salinity Anomaly" of the late 1960s and early 1970s. Atmospheric pressure data are used here to show that the local forcing of high-latitude North Atlantic Ocean fluctuations is augmented by antecedent atmospheric circulation anomalies over the central Arctic. These circulation anomalies are consistent with enhanced wind-forcing of thicker, older ice into the Transpolar Drift Stream and an enhanced export of sea ice (fresh water) from the Arctic into the Greenland Sea prior to major episodes of ice severity in the Greenland and Iceland seas. An index of the pressure difference between southern Greenland and the Arctic–Asian coast reached its highest value of the twentieth century during the middle-to-late 1960s, the approximate time of the earliest observational documentation of the Great Salinity Anomaly.

1. Background

A climatic event that has received increasing attention recently is the so-called "Great Salinity Anomaly" in the high latitudes of the North Atlantic Ocean. This anomaly developed over a succession of years in the 1960s. As shown in Fig. 1 (from Dickson et al. 1988), the anomaly was apparent during the late 1960s in the Greenland Sea and appears to have propagated with the prevailing ocean currents into the Labrador Sea in 1971–72. Oceanographic data suggest that the anomaly was then advected across the North Atlantic by the end of the 1970s. Manifestations of this event in the Greenland, Iceland, and Labrador seas were negative salinity anomalies of −0.1 to −0.5 ppt in the upper 100 m, together with water temperature anomalies of −1° to −2°C (Dickson et al. 1988). The salinity anomaly was also accompanied by large positive anomalies of sea ice coverage (Fig. 2). Mysak and Manak (1989) have illustrated the advective propagation of the sea ice anomaly, in phase with the salinity anomaly, from the Greenland Sea in 1968–69 to the Labrador Sea in 1971–72. Mysak et al. (1990) present additional evidence that the 3–4 year time scale is characteristic of anomaly propagation between these two seas.

Because of its magnitude and time scale, the Great Salinity Anomaly may represent the second largest signal—after the ENSO signal—in the ocean climate system (Aagaard 1989, personal communication). The event has major climatic implications because the North Atlantic subpolar region is the major source of deep ocean water. More specifically, the oceanic convection that occurs in the vicinity of the Greenland and Iceland seas is of major importance to the Atlantic and global thermohaline circulation (Aagaard and Carmack 1989; Broecker et al. 1985; Aagaard et al. 1985). Because the major convective gyres of the Greenland, Iceland, and Norwegian seas (and the Labrador Sea) are very weakly stratified, these regions are "rather delicately poised with respect to their ability to sustain convection" (Aagaard and Carmack 1989, p. 14 495). The same authors suggest that the Great Salinity Anomaly may represent a "small-scale analog" to past climatic regimes in which North Atlantic deep convection was effectively suppressed by a freshening of the surface waters in this region. The physical significance of the negative salinity anomalies stems from the fact that the density of sea water is almost entirely salinity-controlled at temperatures close to the freezing point. The existence of more than one stable ocean–atmosphere climatic regime, depending on the occurrence or nonoccurrence of convection in the high-latitude North Atlantic, has been suggested by paleoclimatic analyses (Broecker and Denton 1989), by ocean model experiments (Bryan 1986), and by recent global atmosphere–ocean model experiments (Manabe and Stouffer 1988).

In view of the potential climatic importance of the Great Salinity Anomaly, the origin of the anomaly becomes a key issue. Aagaard and Carmack (1989) have

Corresponding author address: John E. Walsh, Department of Atmospheric Sciences, 105 South Gregory Avenue, University of Illinois, Urbana, IL 61801.

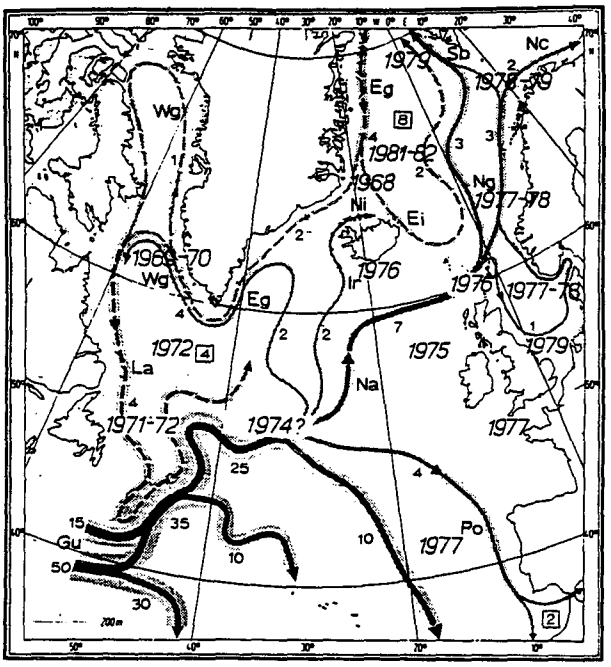

FIG. 1. Dates of North Atlantic salinity minimum superimposed by Dickson et al. on Dietrich et al.'s (1975) transport scheme for the North Atlantic (from Dickson et al. 1988, Fig. 7).

recently constructed a fresh-water budget for the seas surrounding Greenland, Iceland, and Norway. Because the dominant sources of fresh water are the influxes of ice and water through the Fram Strait, Aagaard and Carmack argue that the variability of the outflow from the Arctic Ocean may be largely responsible for the Great Salinity Anomaly. This hypothesis differs from Dickson et al.'s (1988) argument that more localized wind anomalies over the Greenland Sea explain the salinity anomaly. A third hypothesis is that differences between evaporation and precipitation may be responsible for the anomaly (Pollard and Pu 1985).

This note describes some preliminary results in support of the notion that variable ice export contributes to anomalies of temperature and salinity in the North Atlantic. High-latitude circulation anomalies are examined in the context of 20th-century Greenland and Iceland sea ice anomalies, particularly those of the late 1960s. The motivation for the examination of atmospheric circulation (sea level pressure) data is that anomalies of sea ice drift and upper-ocean currents are determined largely by surface wind anomalies. Thorndike and Colony (1982), for example, show that large fractions ($\geq$80%) of the variance of sea ice drift in the central Arctic can be explained by the sea level pressure field. While the ocean currents become increasingly important as the ice drifts into Fram Strait, short-term anomalies of geostrophic wind are significantly correlated with ice drift even in the Greenland Sea (Thorndike and Colony 1982, their Fig. 4; Moritz 1988, his Fig. 4.13). Kelly et al. (1987) have shown that these correlations extend to the seasonal time scale in the Icelandic region. The present study extends Kelly et al.'s analysis to the longer (multiyear) time scales characteristic of the drift of sea ice across the Arctic from the primary regions of ice growth along the Siberian shelf (Fig. 3). The specific hypothesis is that atmospheric pressure fluctuations over areas of the Arctic other than the Greenland and Iceland seas may contribute to anomalies of sea ice (and, implicitly, upper-ocean salinity) in the waters east of Greenland. The postulated link between the larger-scale atmospheric circulation and upper-ocean fluctuations east of Greenland is the Transpolar Drift Stream (Fig. 3) and its transport of fresh water (sea ice) from the Arctic into the Greenland Sea.

The computations summarized below were performed in order to address several key questions:

1) What are the temporal scales of the atmospheric circulation anomalies relevant to sea ice anomalies in the Greenland–Iceland region?
2) What is the spatial character of the associated atmospheric forcing?
3) Does the record of high-latitude atmospheric variations indicate a "uniqueness" (at least during the twentieth century) of the Great Salinity Anomaly?

2. Data

The computations are based primarily on monthly grids of sea level pressure for the period 1899–1980, an annual index of sea ice severity north of Iceland for the same period (Kelly et al. 1987), and the ocean temperature and salinity anomalies at 25 m depth for 1950–1974 in the Iceland–Jan Mayen region, 67°–69°N, 11°–15°W (from Malmberg 1973; updated by Dickson et al. 1988).

The sea level pressure data are the Northern Hemisphere 5° × 5° latitude–longitude grids archived at the National Center for Atmospheric Research (NCAR). The monthly grids are based primarily on the daily or twice-daily analyses of the U.S. Navy and the National Meteorological Center (including its predecessor agencies). A detailed assessment of the NCAR dataset has been provided by Trenberth and Paolino (1980). Jones (1987) has evaluated the biases and errors in analyzed Arctic pressures for a slightly longer (1873–1981) dataset, much of which contains the same analyses as the NCAR series. Both of these assessments indicate that the analyzed sea level pressures in the central Arctic Ocean were spuriously high until the 1930s. The magnitudes of this bias exceed 5 mb in the Canadian side of the Arctic Ocean (Jones 1987, his Fig. 9). An additional bias over the Alaska–Yukon region of northwestern North America was found by Trenberth and Paolino and confirmed by Jones. This bias was attributed to an erroneous station elevation and resulted in errors of up to 10 mb during the first two decades of the 1900s. Neither study found indications of a major

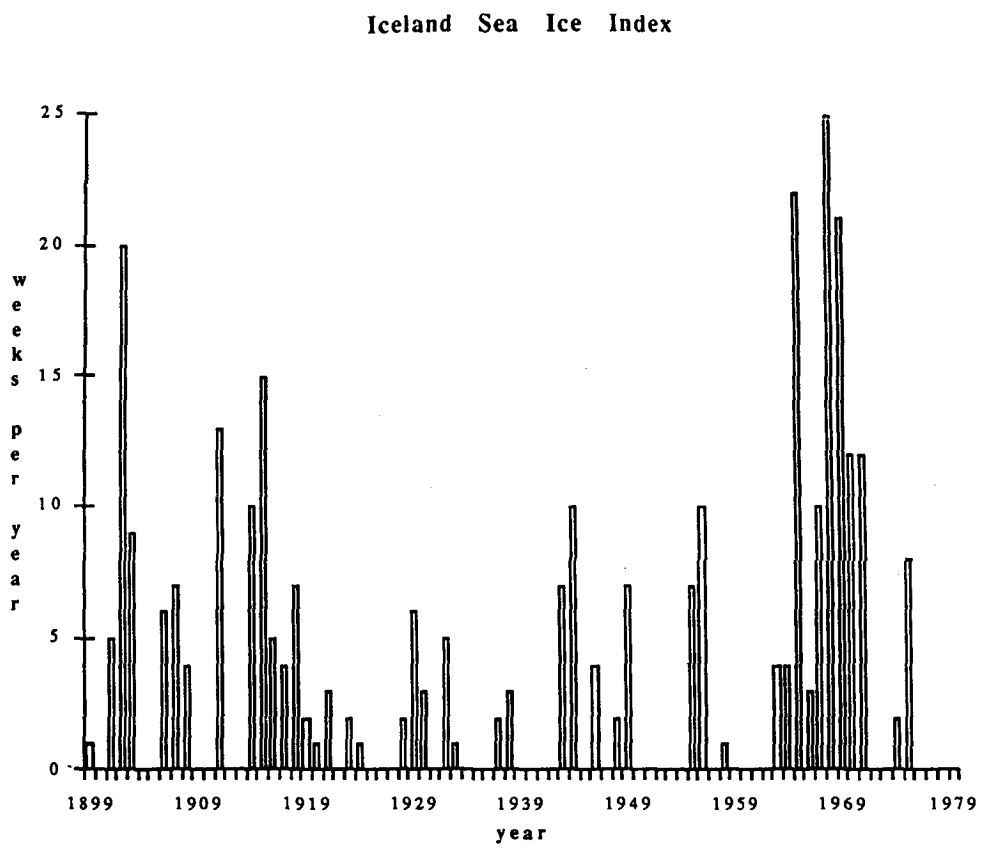

FIG. 2. Index of sea ice severity north of Iceland. Date indicates calendar year in which winter ends (from Kelly et al. 1987, Fig. 2).

bias in the Atlantic subpolar region or the Eurasian coastal region, which will be the focal points of the data analysis described below. In view of these earlier assessments, present inferences pertaining to the central Arctic Ocean are based largely on the post-1940 subset of the data.

The sea ice index used by Kelly et al. (1987) is based on the compilation by Koch (1945) and subsequent updates (see Lamb 1977). The index is essentially the number of weeks in which the northern coast of Iceland was affected by sea ice in a particular ice year (e.g., October–June). While this index is not necessarily an optimal measure of areal ice coverage (or other oceanographic variables) in the east Greenland region, it clearly indicates that the 1968–1972 period of the Great Salinity Anomaly was unique in terms of Icelandic ice severity, at least for the twentieth century (Fig. 2). The most likely drawback of the use of this index is that short-term (on the order of weeks) anomalies of northwesterly winds may occasionally advect ice into Icelandic coastal waters, even though the longer-term (seasons) oceanographic impacts of these anomalies may be negligible.

Malmberg's (1973) ocean temperature and salinity data are in the form of anomalies at 25-m depth for the month of June. The measurements were obtained at hydrographic stations between Iceland and Jan Mayen during the period 1950–1973. Updated annual time series of the two variables are shown by Dickson et al. (1988, their Fig. 5).

3. Results

As an illustration of the spatial scales of the fluctuations of interest, Fig. 4 shows the mean departures from normal (1952–1988) sea level pressure for the 12-month period, April 1967–March 1968, prior to the maximum of the Icelandic sea ice index in Fig. 2. Figure 1 indicates that the Great Salinity Anomaly was present in the Greenland Sea during 1968. Pressures during the 12-month period were above normal to the south of Greenland and Iceland, as found by Kelly et al. (1987) in their analysis of composites of severe and light ice years north of Iceland. However, unlike the Kelly et al. composites, the dominant feature of the anomaly field in Fig. 4 is the region of below-normal pressures (5–6 mb north of the Asian coast). The anomalous component of the geostrophic wind in the vicinity of Fram Strait and Svalbard is consistent with an above-normal outflow velocity of sea ice, since the

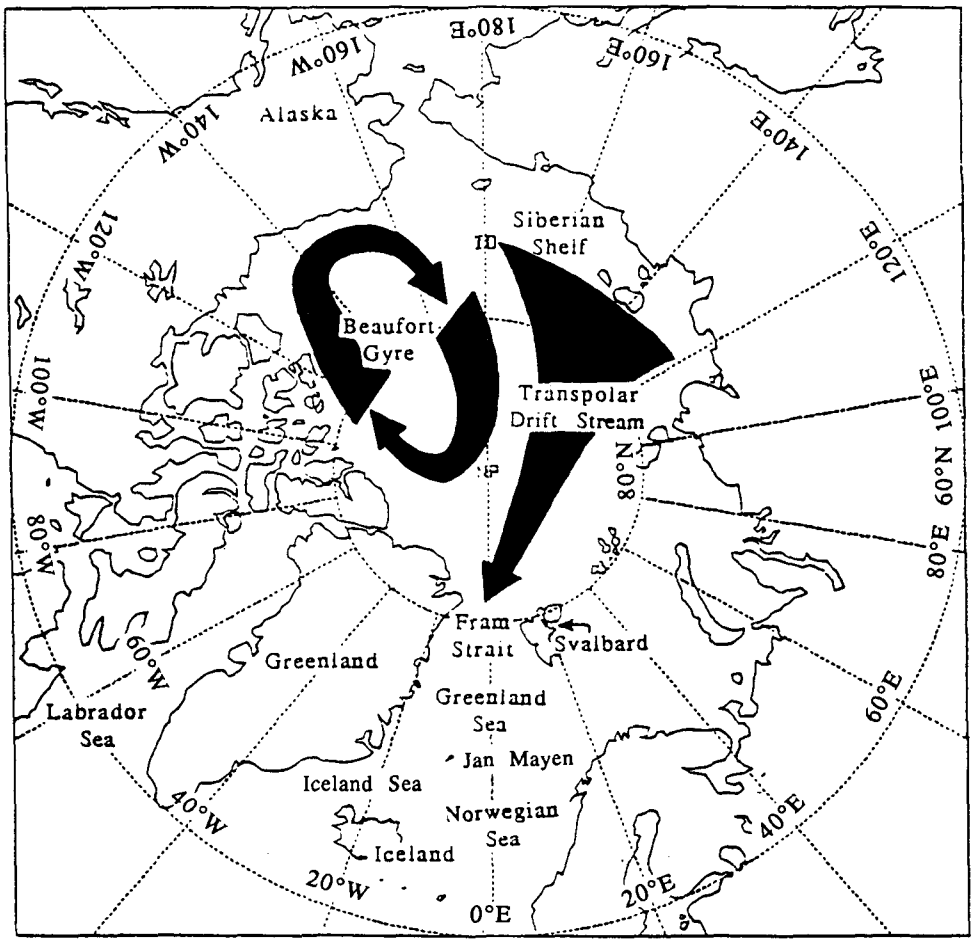

FIG. 3. General pattern of sea ice drift in the Arctic Ocean. Place names mentioned in text are also shown.

gradient of the pressure anomaly contours is in the same general direction as the gradient of the climatological normals. However, poleward of Fram Strait the anomalous component of the geostrophic wind is less parallel to the Transpolar Drift Stream. The anomalous wind forcing inferred from Fig. 4 is such that ice from the waters offshore of northwestern Canada and Greenland would be advected into the outflow region. As shown in Fig. 5 (from Bourke and Garrett 1987), these waters contain the thickest sea ice in the Arctic. The anomaly pattern of Fig. 4 therefore implies stronger or more frequent incursions of thick (old) sea ice into the Transpolar Drift Stream. The climatological normal component of the wind forcing, upon which the anomaly field of Fig. 4 is superimposed, will then lead to a greater-than-normal export of fresh water into Fram Strait. This mechanism differs somewhat from the postulate of a simple acceleration of ice velocities in the Transpolar Drift Stream, but it is nevertheless consistent with an enhanced flux of low-salinity water (sea ice) into the Greenland Sea. The pattern in Fig. 4 also suggests the possibility of an extrusion of Arctic halocline water toward the periphery of the Arctic. An enhanced flux of the relatively fresh near-surface waters into the subarctic seas would reinforce the effect of the sea ice export. However, the response of the Arctic halocline to perturbations of surface forcing over these time scales is highly uncertain. The present understanding of the mechanisms by which the Arctic halocline is maintained is incomplete, and the investigation of these mechanisms is a high priority of upcoming programs in Arctic System Science (NSF 1990).

In order to place Fig. 4 into a longer-term framework, Fig. 6 shows the correlations between the Icelandic sea ice index and the 12-month means (April–March) of the sea level pressures for the period 1941–1980. The correlation pattern in the eastern Arctic is dominated by two features, one to the south of Greenland and one to the Eurasian side of the Pole. The former corresponds to the major feature of Kelly et al.'s (1987) composite anomaly fields, while the latter is northeast of a secondary feature suggested by some of Kelly et al.'s seasonal plots. The two features are found in Lau and Nath's (1990, their Fig. 2) first rotated principal

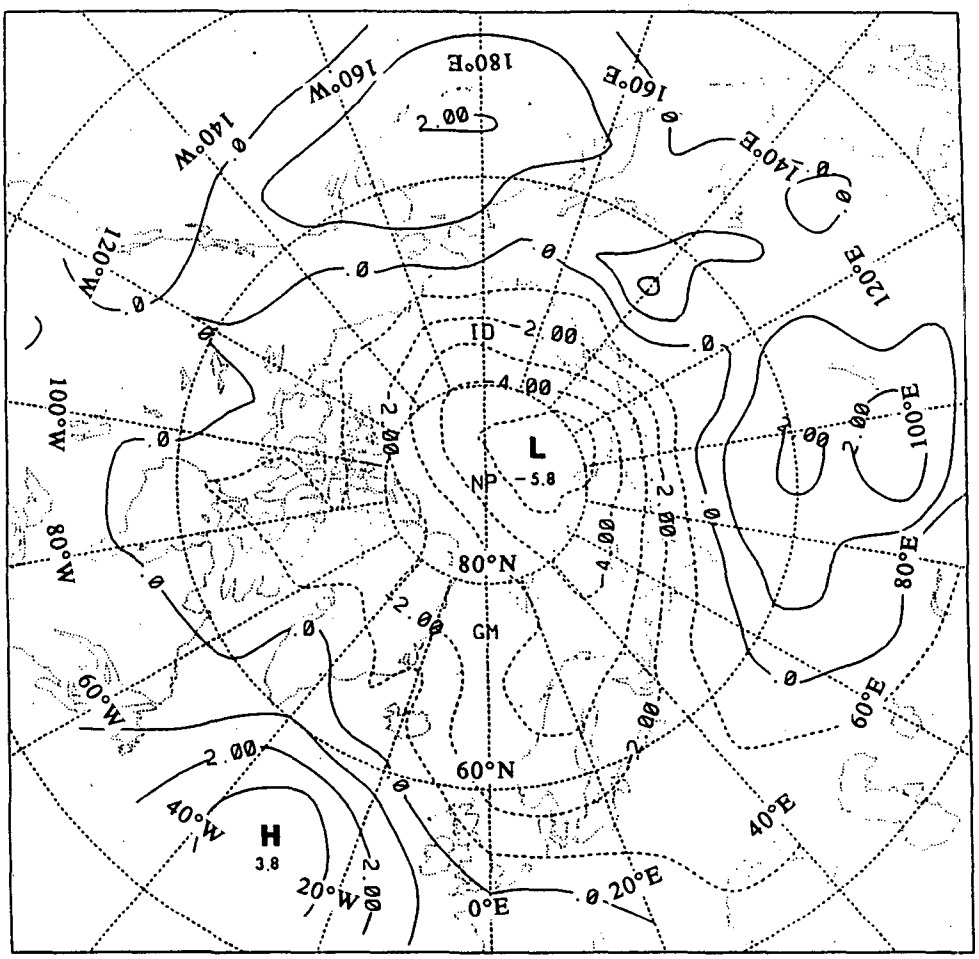

FIG. 4. Departure from normal sea level pressure (mb) averaged over 12-month period, April 1967–March 1968.

component of Northern Hemisphere midtropospheric geopotential, although the Arctic feature is often not present in depictions of the North Atlantic Oscillation in the midtroposphere (e.g., Barnston and Livezey 1987, their Fig. 2). The same spatial pattern appears in the correlation fields based on the 12-month (April–March) pressures for all 82 years, 1899–1980, although the central values of the major features are slightly smaller: the maximum south of Greenland decreases from 0.51 to 0.38, and the minimum north of Eurasia weakens from −0.33 to −0.26. While these point-values are statistically significant at the 95% level if successive years are assumed to be independent, the level of field significance depends strongly on the somewhat arbitrary definition of the field "boundaries." It should be noted that the Greenland feature is in a region of relatively consistent station data coverage throughout the 82-year period, while the region north of Eurasia suffers from data uncertainties, especially in the 1899–1939 period. As documented by Jones (1987, his Table 1), the key stations for the Eurasian Arctic pressure analyses and the initial years of their records are Vardo (70°N, 31°E), 1861; Verkhoyansk (68°N, 133°E), 1910; and Salekhard (67°N, 67°E), 1887. Other stations having less complete records are Ostrov Dikson (74°N, 80°E), 1917; Mayle Karamakuly (72°N, 53°E), 1897; and Anadyr (65°N, 178°E), 1926. Statistics of pressure fluctuations poleward of ~75°N in the Eurasian Arctic during the earlier decades are therefore questionable.

The anomalous component of the gradient wind is not strictly parallel to the pressure-correlation isopleths (e.g., Fig. 6) because the standard deviation of pressure shows some spatial variation. However, composite fields of pressure anomalies corresponding to Fig. 6 show a pattern very similar to that of Fig. 6 in the Arctic. Figure 7, for example, shows a composite field of the 12-month (April–March) pressure anomalies weighted according to Malmberg's (1973) salinity anomalies at 25 m in the Iceland–Jan Mayen region. (The weights were normalized so that they sum to unity.) The similarity of the Arctic patterns of Figs. 6

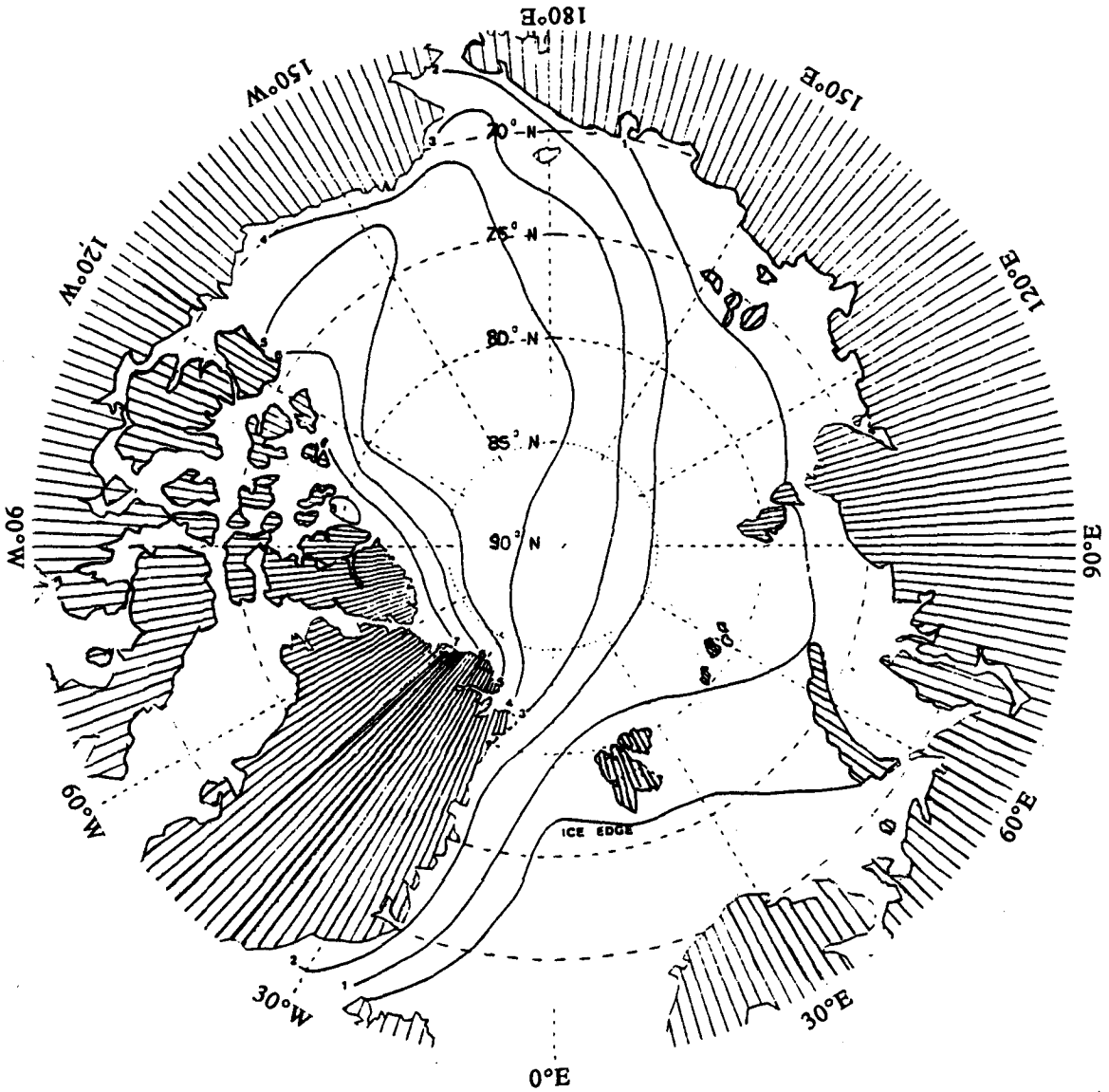

FIG. 5. Mean ice draft (m) in winter derived from a composite of submarine underice sonar data (from Bourke and Garrett 1987, Fig. 5).

and 7 implies that correlation fields are interpretable in terms of gradient wind anomalies. The fact that Figs. 6 and 7 are based on different oceanic variables (sea ice and salinity, respectively) indicates that the sea ice index is indeed a reasonable proxy for the salinity anomaly in the Iceland–Jan Mayen region.

As the length of the averaging period of the pressure anomalies increases, two tendencies are apparent. First, the magnitude of the correlation with pressures in the Arctic–Asian region increases relative to the correlation with pressures south of Greenland. (The center of the Arctic–Asian feature also shifts to the Asian coast.) Figure 8 shows the pressure-averaging-period dependence of the central values of the two major correlation features obtained using the entire 82 years of data. (The southern Greenland and Arctic–Asian "centers" were required to be within 10° latitude and 45° longitude of 65°N, 45°W and 70°N, 150°E, respectively.) When the number of months in the pressure-averaging period (ending in March of the year of the ice index) reaches 18, the magnitude of the Arctic–Asian correlations exceeds the magnitude of the southern Greenland correlations. Second, the contours of the correlation pattern become more nearly perpendicular to the Transpolar Drift Stream as the pressure-averaging period increases. As shown in Fig. 9 for the correlations based on the antecedent 30 months of pressure anomaly data, the correlation pattern implies anomalous airflow

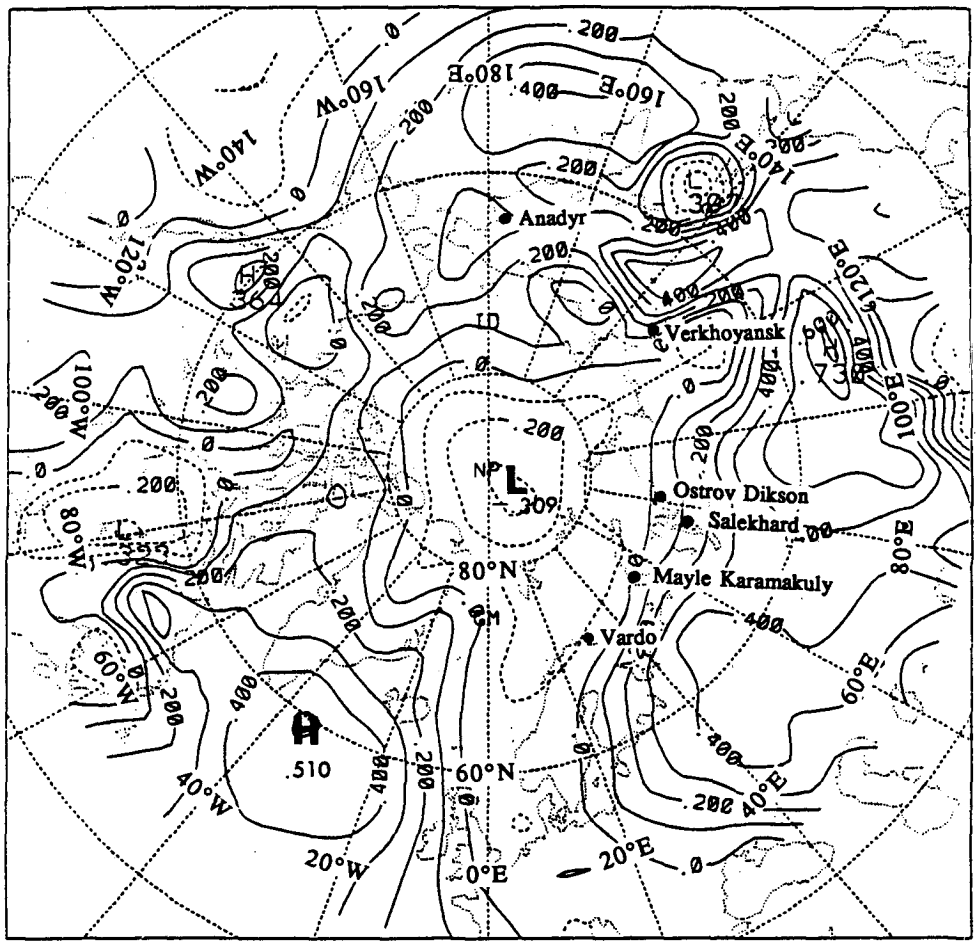

FIG. 6. Correlations between sea ice index and antecedent 12-month (April–March) sea level pressures for the 1940–1980 subperiod.

(wind stress) from the region of thickest ice directly into the transpolar drift. The pattern in Fig. 9 is also quite consistent with the pressure anomaly plot for the early period of the Great Salinity Anomaly (Fig. 4). Both figures suggest that there is an enhanced flux of low-salinity water (sea ice) into the Greenland Sea prior to a period of severe ice conditions in the Greenland and Iceland seas. The results imply that the appropriate time scale for this type of interregional association is one-to-several years.

These results do not imply that local forcing in the East Greenland area is of secondary importance. To the contrary, the southern Greenland center is the most prominent feature of the 12-month pressure correlation with sea ice and ocean salinity (Figs. 6 and 7). The geostrophic wind anomalies associated with this feature imply advection of ice from the Greenland Sea toward Iceland. Positive pressure anomalies southeast of Greenland are likely to be a necessary condition for upper ocean anomalies north of Iceland. The Arctic contribution diagnosed here may thus be regarded as a remote "boost," over longer time scales, to a dominant local forcing.

The above interpretation is reinforced by the fact that the southern Greenland correlation in Fig. 8 does not continue to decrease beyond 24 months. Rather, as shown in Fig. 8, it increases somewhat when the averaging period is increased beyond 24 months. This behavior raises the possibility that the Arctic feature is not independent of, but perhaps teleconnected to, the Greenland feature at the longer time scales. In order to address this possibility, partial correlations (e.g., Panofsky and Brier 1958) between pressure and the sea ice index were computed by first removing the pressure variance associated with the southern Greenland point (65°N, 40°W). The partial correlation fields (not shown) contain centers of negative values over the same Asian coastal regions as do the full correlation fields, as well as the same general pattern in the central Arctic as does Fig. 9. This implies that there is enhanced advection of thick ice into the Transpolar Drift Stream–or *less* than normal advection of thick ice *from* the

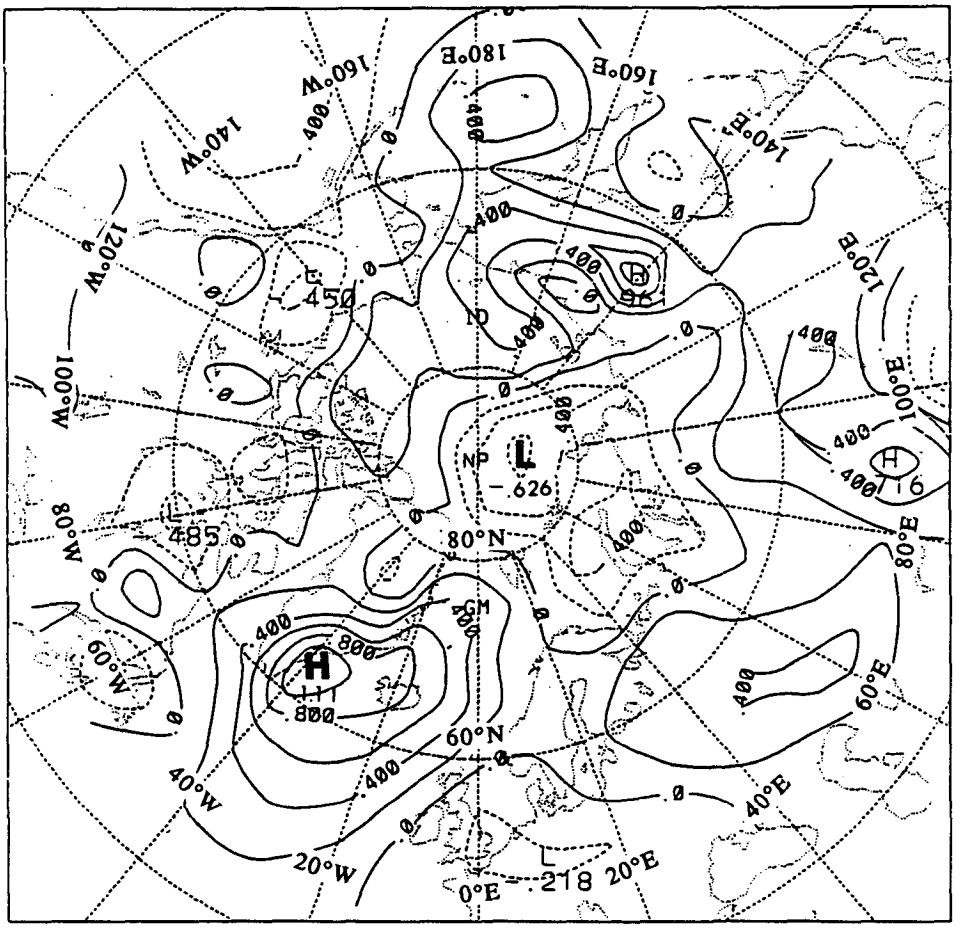

FIG. 7. Anomalies of antecedent 12-month (April–March) average sea level pressure weighted by negative of salinity anomaly in Iceland–Jan Mayen region. Weights were normalized to a sum of unity.

Transpolar Drift Stream into the Canadian Arctic. The Arctic–Asian *partial* correlations are shown in Fig. 8 (solid circles) for the grid points and averaging periods corresponding directly to the Arctic–Asian total correlations on the dashed line. Also shown in Fig. 8 (open circles) are the maximum partial correlations in the Arctic–Asian region for specific 6-month subperiods. (Total correlations of the Greenland pressures for 6-month subperiods are not shown because centers near southern Greenland were not identifiable in several of the subperiods.) The Arctic–Asian partial correlations for 6-month periods (open circles in Fig. 8) exceed the corresponding total correlations out to 24 months, after which they precipitously decrease. This reinforces the idea that the Arctic advective mechanism is operating independently of the local forcing at lags of 1½–2 years. The partial values for cumulative periods 18–30 months (solid circles in Fig. 8) are smaller than the corresponding total correlations by 0.05–0.10. This implied weak correlation between the Arctic–Asian and Greenland features is also apparent in teleconnection fields based on the correlations between the pressure anomalies over southern Greenland (65°N, 40°W) and the pressure anomalies elsewhere. The correlations between this southern Greenland point and the Arctic–Asian point (70°N, 150°E) used for the index described below were found to be +0.18, −0.08, −0.20, −0.22, and −0.26 for averaging periods of 12, 24, 36, 48, and 60 months. The above magnitudes are such that teleconnections to the southern Greenland point can explain only a small part of the Arctic–Asian correlations over any averaging period ≤ 60 months. Nevertheless, they are large enough to explain the small increase in the Greenland point's correlation after 24 months (Fig. 8).

Finally, an attempt is made to place the Great Salinity Anomaly into a temporal perspective by showing a time series of the pressure differences between southern Greenland (65°N, 40°W) and the Arctic–Asian coast (70°N, 150°E). These two points are the approximate centers of the pressure-ice correlation fields based on the longer pressure-averaging periods (e.g.,

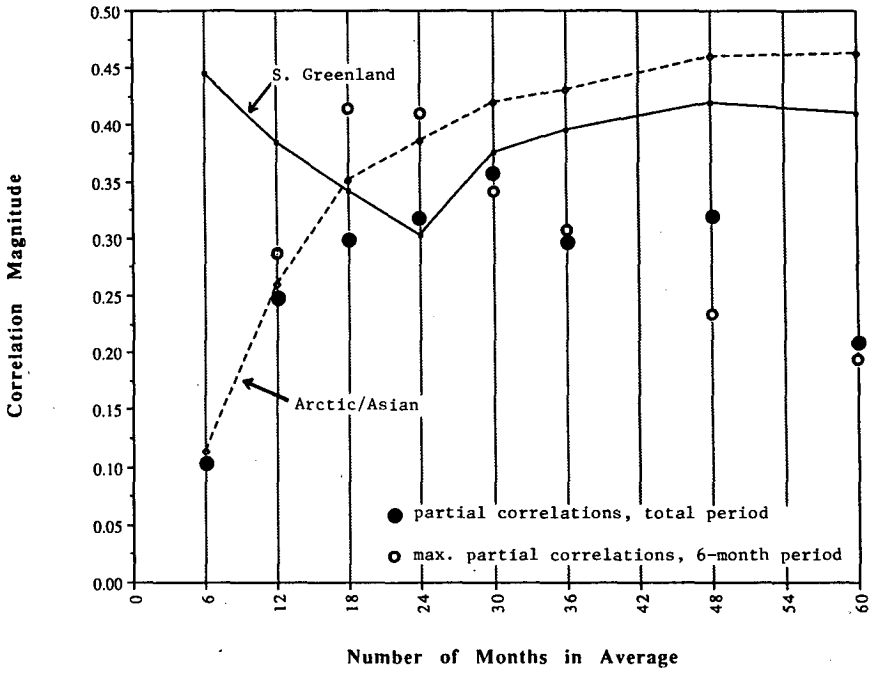

FIG. 8. Maximum magnitudes of correlations between sea ice index and antecedent sea level pressure in southern Greenland (solid line) and Arctic–Asian coastal region (dashed line). Abscissa is number of months, prior to March 31, over which pressure anomalies were averaged. Results are based on entire data sample, 1899–1980. Also shown are partial correlations between sea ice index and Arctic–Asian coastal pressure after removal of variance explained by southern Greenland point: solid circles are partial correlations corresponding directly to geographical points and averaging periods of points on dashed line; open circles are maximum partial correlations in Arctic–Asian region for specific 6-month periods (ending with abscissa value).

Fig. 9) and, as described above, the teleconnections between the two points are weak. Figure 10 shows the 60-month running mean of this index for the period 1899–1980. The highest values of the index were reached in the late 1960s. The peak value of the late 1960s exceeds the next largest peak value (~1945) by 2 mb. While the corresponding time series of the single-point pressures for southern Greenland (65°N, 40°W) also reaches its twentieth-century peak in 1969, other relative maxima (e.g., 1982) in the southern Greenland time series are well within 2 mb of the 1969 peak. Figure 10 indicates that the Great Salinity Anomaly occurred subsequent to a period that, at least for the twentieth century, was atmospherically unique in the northern high latitudes. The results thus support the notion that the roots of the Great Salinity Anomaly can be traced to the atmospheric circulation not only locally (east of Greenland) but also over the Arctic Ocean.

Figure 10 contains a suggestion of a relatively strong peak of the pressure index in the first few years of the twentieth century. Prior to the 1960s, the twentieth-century peak of the Icelandic sea ice index had occurred in the first few years of the century (Fig. 2). While the data do not permit a meaningful assessment of this earlier event here, Dickson et al. (1988) note that the rather fragmentary ocean data suggest a period of abnormally low salinities in the North Atlantic during the early 1900s.

4. Discussion

The results of the previous section indicate that the Great Salinity Anomaly occurred during and after a period in which the Greenland–Arctic pressure difference reached its highest (least negative) value of the twentieth century. To the extent that the Greenland–Arctic pressure difference is an index of the high-latitude atmospheric circulation, one may conclude that the high-latitude atmospheric circulation was in a highly anomalous state during the late 1960s. The 1967–68 pressure field is consistent with an increase of the ice export through Fram Strait. For 1967–68 and for the longer (1899–1980) record, the data suggest that the increased export of sea ice (fresh water) prior to severe Icelandic ice conditions may be achieved through the export of thicker ice. The latter interpretation admittedly contains a speculative element which, however, can be tested by the monitoring of ice thickness using upward-looking sonar devices now planned

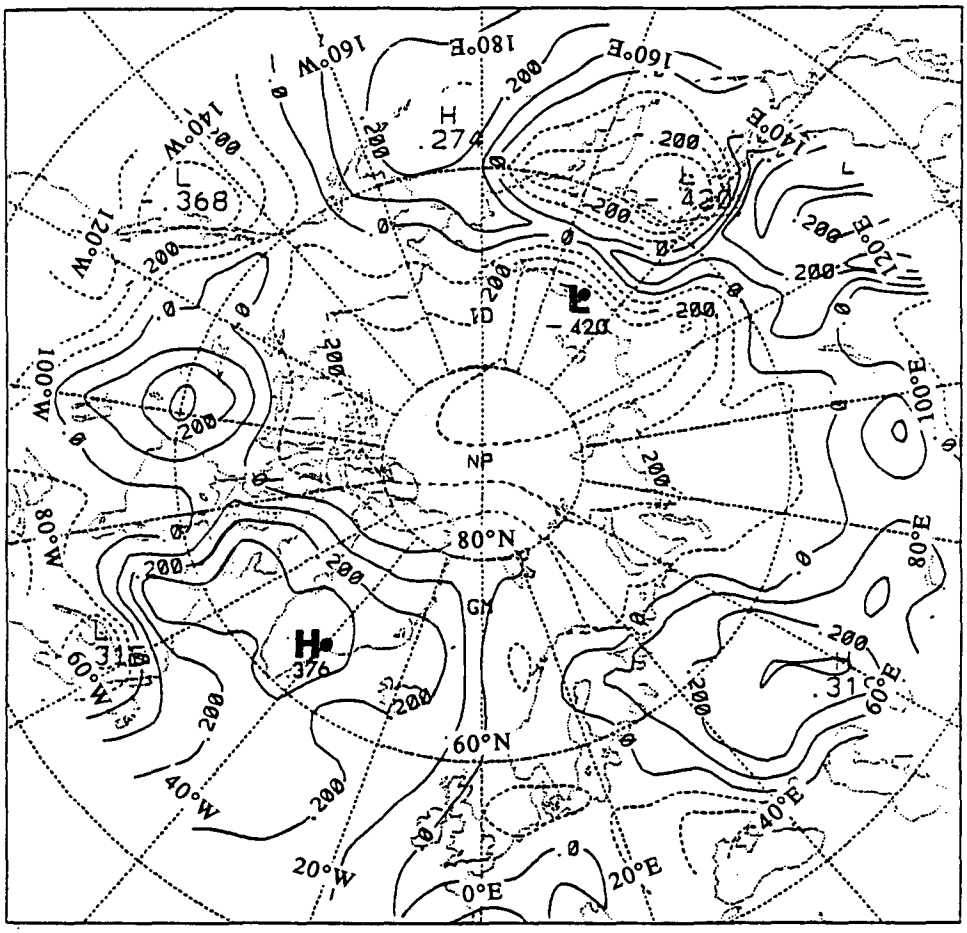

FIG. 9. Correlations between sea ice index and antecedent 30-month (October–March) sea level pressures for the entire data sample, 1899–1980.

for mooring in Fram Strait (Untersteiner 1989, personal communication).

Of the two components of the Greenland–Arctic pressure index, the first represents the strongest and physically most direct link to the sea ice index. Positive pressure anomalies over southern Greenland correspond to advection of sea ice anomalies and/or colder, fresher water toward Iceland, as argued by Dickson et al. (1988). The Arctic component is somewhat less robust, but it 1) appears to be largely independent of the Greenland component, 2) enhances the uniqueness of the period preceding the Great Salinity Anomaly, and 3) has a corresponding physical basis in the variability of the export of sea ice from the central Arctic to the Greenland Sea. In view of 2), it appears that the Arctic component of the forcing provides a "remote boost" to the local forcing in the sense that the strongest oceanic impacts (e.g., a "Great Salinity Anomaly") will result when the phasing of *both* the local and the remote forcing is favorable. An enhanced outflow of Arctic ice *without* favorable local forcing east of Greenland will evidently not result in noteworthy anomalies of ocean temperature and salinity. This interpretation is consistent with the finding that the sea ice correlations with the central Arctic pressures are weaker than those with the Greenland pressures over relatively short periods ($\leq$12 months). On the other hand, Figs. 4 and 8 and present experiments with alternative pressure indices suggest that favorable local forcing may not result in a once-in-a-century North Atlantic ocean anomaly without the contribution of enhanced ice export from the Arctic.

The results raise the possibility that major North Atlantic sea ice and ocean anomalies should be viewed in the context of atmospheric fluctuations over a larger high-latitude area than the Greenland–Iceland region. The correlations ($r \sim 0.4$–0.5) between the sea ice index and Arctic pressure anomalies are admittedly not large. However, the results may underestimate the signal in view of 1) the limitations on the data, especially for Arctic pressure, and 2) the fact that our computations included only a few averaging lengths and ending months of the atmospheric data. The results do appear to merit further investigation in the context

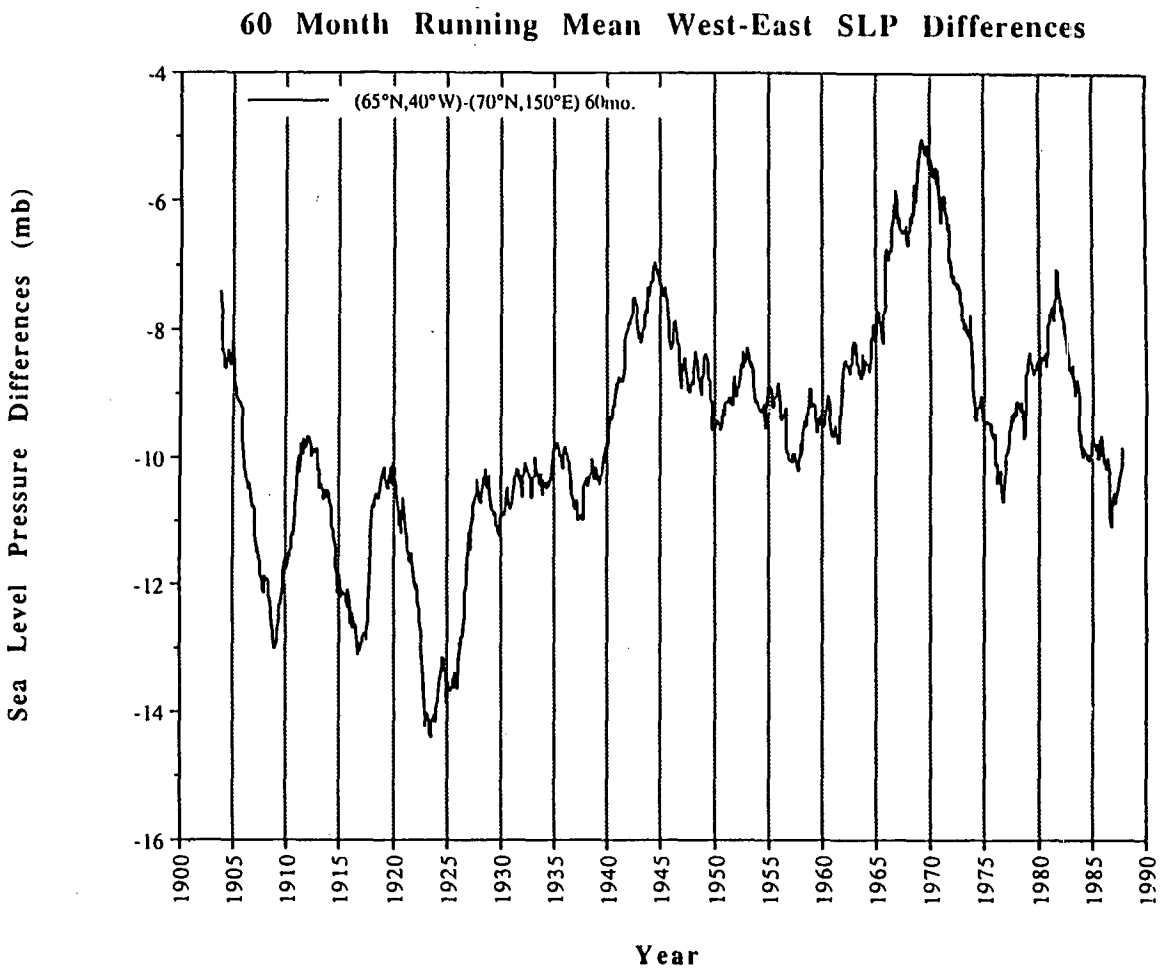

FIG. 10. Five-year running mean difference of sea level pressure between southern Greenland (65°N, 40°W) and northern Asian coast (70°N, 150°E). Abscissa denotes end of 60-month period.

of larger projects such as NOAA's Atlantic Climate Change Program (ACCP).

Finally, it is noted that associative–correlative results such as those presented here do not represent evidence of causality. The results are consistent with the hypothesis that advective forcing from the Arctic is a factor contributing to upper-ocean variability in the North Atlantic. However, since correlation is no guarantee of causality, it is quite possible that the ocean variations and the Arctic pressure variations are both responses to forcing from elsewhere in the climate system. There is also the intriguing possibility that the ice–ocean fluctuations in the Iceland–Greenland region contribute significantly to the atmospheric fluctuations in high latitudes, thereby resulting in statistical associations such as those obtained here. While this possibility is acknowledged, it is considered rather unlikely because 1) the results in Figs. 6–10 are more indicative of a positive lag of the ice fluctuations relative to the atmospheric variations, and 2) other empirical and modeling studies indicate that the North Atlantic sea surface anomalies most pertinent to atmospheric forcing are those in the waters southeast of Newfoundland (Ratcliffe and Murray 1970; Palmer and Sun 1985).

Acknowledgments. This work was supported by NASA's Interdisciplinary Research Program through Grant IDP-88-009 and by the National Science Foundation, Climate Dynamics Program, through Grant ATM-8808192. We thank Norene McGhiey for typing the manuscript.

REFERENCES

Aagaard, K., and E. C. Carmack, 1989: The role of sea ice and other fresh waters in the Arctic circulation. *J. Geophys. Res.*, **94,** 14 485–14 498.

——, J. H. Swift and E. C. Carmack, 1985: Thermohaline circulation in the Arctic Mediterranean seas. *J. Geophys. Res.*, **90,** 4833–4846.

Barnston, A. G., and R. E. Livezey, 1987: Classification, seasonality, and persistence of low-frequency atmospheric circulation patterns. *Mon. Wea. Rev.*, **115,** 1083–1126.

Bourke, R. H., and R. P. Garrett, 1987: Sea ice thickness distribution in the Arctic Ocean. *Cold Reg. Sci. Technol.* **13,** 259–280.

Broecker, W. S., and G. H. Denton, 1989: The role of ocean–atmosphere reorganizations in glacial cycles. *Geochim. Cosmochim. Acta,* **53,** 2465–2501.

——, D. M. Peteet and D. Rind, 1985: Does the ocean–atmosphere system have more than one stable mode of operation? *Nature,* **315,** 21–26.

Bryan, F., 1986: High-latitude salinity effects and interhemispheric thermohaline circulations. *Nature,* **323,** 301–304.

Dickson, R. R., J. Meincke, S.-A. Malmberg and A. J. Lee, 1988: The "Great Salinity Anomaly" in the northern North Atlantic, 1968–1982, *Progr. Oceanogr.,* **20,** 103–151.

Dietrich, G., W. Kalle, W. Krauss and G. Siedler, 1975: *General Oceanography,* 2nd ed., John Wiley and Sons, 626 pp.

Jones, P. D., 1987: The early twentieth century Arctic high—fact or fiction? *Clim. Dyn.,* **1,** 63–75.

Kelly, P. M., C. M. Goodess and B. S. G. Cherry, 1987: The interpretation of the Icelandic sea ice record. *J. Geophys. Res.,* **92,** 10 835–10 843.

Koch, L., 1945: The East Greenland ice. *Medd. Groenl.,* **130,** 1–374.

Lamb, H. H., 1977: *Climate: Present, Past, and Future. Vol. 2: Climatic History and the Future,* Methuen, 835 pp.

Lau, N.-C., and M. J. Nath, 1990: A general circulation model study of the atmospheric response to extratropical SST anomalies observed in 1950–79. *J. Climate,* **4,** 965–989.

Malmberg, S.-A., 1973: Astand sjavar milli Islands og Jan Mayen, 1950–72. *Aegir,* **66,** 146–148.

Manabe, S., and R. Stouffer, 1988: Two stable equilibria of a coupled ocean–atmosphere model. *J. Climate,* **1,** 841–866.

Moritz, R. E., 1988: The ice budget of the Greenland Sea. Tech. Rept. APL-UW TR8812. 117 pp. [Available from Appl. Phys. Lab., University of Washington, Seattle.]

Mysak, L. A., and D. K. Manak, 1989: Arctic sea ice extent and anomalies, 1953–1984. *Atmosphere: Atmos.-Ocean,* **27,** 376–405.

——, —— and R. F. Marsden, 1990: Sea ice anomalies in the Greenland and Labrador Seas during 1901–1984 and their relation to an interdecadal Arctic climate cycle. *Clim. Dyn.,* in press.

National Science Foundation, 1990: Arctic System Science. *Workshop on Ocean–Atmosphere–Ice Interactions,* Washington, DC, Joint Oceanographic Institutions, Inc., 114 pp.

Palmer, T. N., and Z. Sun, 1985: A modeling and observational study of the relationship between sea surface temperatures and the atmospheric circulation in the northwest North Atlantic. *Quart. J. Roy. Meteor. Soc.,* **111,** 947–975.

Panofsky, H. A., and G. W. Brier, 1958: *Some Applications of Statistics to Meteorology.* Penn. State Univ. Press, 224 pp.

Pollard, R. T., and S. Pu, 1985: Structure and circulation of the upper Atlantic Ocean northeast of the Azores. *Progr. Oceanogr.,* **14,** 443–462.

Ratcliffe, R. A. S., and R. Murray, 1970: New lag associations between North Atlantic sea surface temperatures and European pressure applied to long-range weather forecasting. *Quart. J. Roy. Meteor. Soc.,* **96,** 226–246.

Thorndike, A. S., and R. Colony, 1982: Sea ice motion in response to geostrophic winds. *J. Geophys. Res.,* **87,** 5845–5852.

Trenberth, K. E., and D. A. Paolino, 1980: The Northern Hemisphere sea level pressure dataset: trends, errors, and discontinuities. *Mon. Wea. Rev.,* **108,** 855–872.